Thus the data plotted in Fig. 2 can be collapsed to a single curve by defining a reduced frequency which references the screech to a jet at an arbitrary total temperature

$$f_r = f_{T_0}[(T_{amb} + T_e)_{T_r}/(T_{amb} + T_e)_{T_0}]^{1/2} \quad (4)$$

where f_r = reduced frequency, f_{T_0} = actual frequency at T_0, T_r = reference total temperature. Figure 3 displays the reduced frequencies for the three total temperatures investigated and a reference total temperature, $T_r = 65^0$F. Use of Eq. (4) collapses the data to a band which is bound by the screech associated with $T_0 = 65^0$F. Since no simple temperature dependence can narrow these boundaries, the presented dependence is considered adequate. Equation (3) is also plotted on this figure with values: $K_4 = 8.0 \times 10^{-2}$, $K_5 = 0.40$.

Conclusions

This investigation has quantified the dependence of jet screech on temperature for an axisymmetric, sonic jet. The temperature changes vary the characteristic velocity which was found to be the sound speed in the shear layer. The empirical expression of Eq. (3) adequantly represents this dependence with constants $K_4 = 8.0 \times 10^{-2}$ and $K_5 = 0.40$. There are, therefore, three parameters which vary the screech frequency: jet pressure ratio, jet temperature, and jet diameter.

It was observed that an apparent discontinuity in frequency for an ambient temperature jet ($T_0 = 65^0$F) was actually a continuous transition - as the intensity at the lower frequency decreased, the intensity at a higher frequency increased. Such discontinuities were not observed in hotter jets, although related phenomena, such as multiple dominant frequencies, occurred at low pressure ratios.

References

[1] Powell, A., "On the Noise Emanating from a Two-Dimensional Jet Above Critical Pressure," *The Aeronautical Quarterly*, Vol. IV, Feb. 1953, pp. 103-122.

[2] Powell, A., "On the Mechanism of Chocked Jet Noise," *Proceedings of the Physical Society*, Vol. B66, Dec. 1953, pp. 1039-1056.

[3] Merle, M., "Ondes Sonores Emises par un Jet d'air," *Academie des Sciences, Comptes Rendus*, Vol. 240, May 1955, pp. 2055-2057.

Hypersonic Incipient Separation on Delta Wing with Trailing-Edge Flap

Dhanvada M. Rao*
National Aeronautical Laboratory, Bangalore, India

Introduction

RECENT investigations of trailing-edge flap control effectiveness on delta wings at hypersonic Mach numbers have indicated the complexity of the flow patterns associated with flap-induced boundary-layer separation.[1-4] Factors contributing to the complexity are the three-dimensional flow in the delta wing boundary layer and the effects of transition. Under such three-dimensional separated-flow conditions, reliable assessment of flap effectiveness and intense heating rates encountered at re-attachment on the flap pose serious design problems. These difficulties could possibly be overcome by providing larger flap area and reduced control deflections in order to avoid separating the flow, given the ability to predict incipient separation. However, little is known regarding incipient boundary-layer separation in three-dimensional flow; also, whether the extensive two-dimensional data available on wedge-induced separation could be utilized for this purpose needs to be clarified.

Received December 31, 1974; revision received May 23, 1975. This work was supported by the British Ministry of Technology and carried out at the Department of Aeronautics, Imperial College, London during 1967-1970.

Index categories: Supersonic and Hypersonic Flow; Jets, Wakes, and Viscid-Inviscid Flow Interactions; LV/M Aerodynamics.

*Head, Aerodynamics Division. Member AIAA. Now at NASA Langley Research Center, Hampton, Va.

Table 1 Test data on 75° delta wing with trailing-edge flap

Author	Facility	M	R/in.	L in.	Ref.
Rao (1970)	Imperial College Gun Tunnel	8.2	0.22×10^6 -0.3×10^6	4.0,6.5	1
Davies (1970)	NPL Shock Tunnel	8.0	0.12×10^6 -0.2×10^6	2.6,6.4	2
Keyes (1969)	NASA-LRC Blowdown Tunnel	6.0	0.16×10^6 -0.7×10^6	8.0	3

This Note reviews the limited experimental data available on planar delta wings of 75°-swept sharp leading-edges, with full-span trailing-edge flap deflected into the windward flow (see Table 1). The local Reynolds number range between these investigations covered the laminar, transitional, and turbulent conditions (without the use of boundary-layer trips). A comparison of these results with two-dimensional data has led to some interesting conclusions regarding trailing-edge flap-induced incipient separation on delta wings.

Discussion

Incipient separation was determined by plotting the distance to separation X_s (obtained from pressure distributions or Schlieren photographs) against the hinge-line Reynolds number (R_L), for a fixed flap deflection (δ), and extrapolating to the hinge-line (i.e., zero separation length). An example is shown in Fig. 1, where data from the three sources are plotted for $\delta = 10°$, 20°, and 30°. The extent of separation on the delta wing at a given flap angle appears to follow qualitatively the well-known two-dimensional behavior as influenced by local Reynolds number (e.g., Ref. 5). Thus, an initial decrease in X_s with increasing Reynolds number, representative of laminar flow, is followed by a reversal of the trend with the onset of transition starting in the shear layer and progressing upstream to the attached flow. The data from different sources show good agreement even though the local Mach number on the windward surface ranged from about 4.5 to 7.5 due to varying angle of attack, indicating that transitional separation is dominated by Reynolds number and is relatively less sensitive to Mach number in the range encountered here.

Incipient separation data determined for the 75° delta wing are plotted in Fig. 2 as $\delta_i/\sqrt{M}$ vs R_L (δ_i = flap angle for incipient separation), a form that was previously found to correlate the two-dimensional turbulent as well as transitional data separately over a broad Mach number range.[6] The delta wing data, although few, suggest a distinctive correlation of their own, which offers interesting comparisons with the two-dimensional case. In the laminar regime, flap-induced incipient separation on the delta wing is postponed to larger flap deflection (almost by a factor of two) for given local-flow Mach and Reynolds numbers. The sudden rise of $\delta_i/\sqrt{M}$ from the laminar towards the turbulent level parallels the two-dimensional trend, although occurring earlier, as may be anticipated from the well-known reduction in transition Reynolds number due to leading-edge sweep. The Reynolds number range over which delta wing incipient separation displays transitional behavior corroborates the transition Reynolds number for this wing obtained in the same test facility.[7] Turbulent incipient separation on the delta wing appears to be practically indistinguishable from the two-dimensional data.

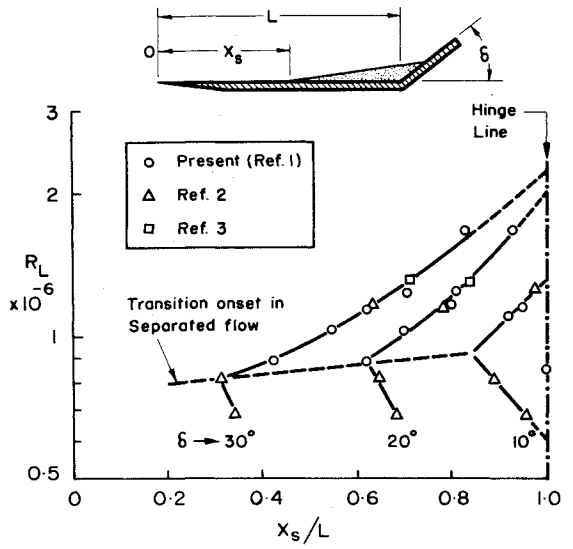

Fig. 1 Center-line separation length on 75° delta with trailing-edge flap.

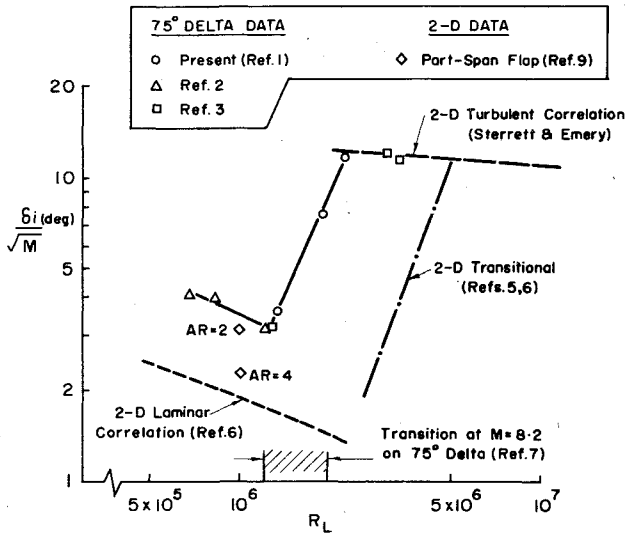

Fig. 2 Correlation of incipient separation due to trailing-edge flap on delta wing.

One may consider two possible factors to explain the observed increase in the flap angle for laminar incipient separation on the delta wing relative to the two-dimensional case. Firstly, there is the nature of the laminar boundary layer on the delta wing. This might be anticipated to be different in structure from the flat-plate boundary layer, because of the cross flows induced near the highly swept leading edges. Detailed velocity profile data on delta wing boundary layers are lacking; however, heat-transfer measurements provide indirect evidence in support of gross similarity between the flat-plate laminar boundary layer and that on the compression surface of a planar delta at small angles of attack (say, less than 10°)[8]

Second, there is a local three-dimensional flow development within the boundary layer when approaching separation, immediately upstream of the hinge line. On the basis of surface oil-flow visualizations, this is believed to take the form of a spanwise outflow in the low-momentum inner layer, resulting in a thinned boundary layer near the hinge line, more resistant to separation (Fig. 3). Such a flow mechanism (analogous to local boundary-layer suction) is believed also to underly the increased flap angle for incipient separation observed with low aspect ratio, finite-span flaps in

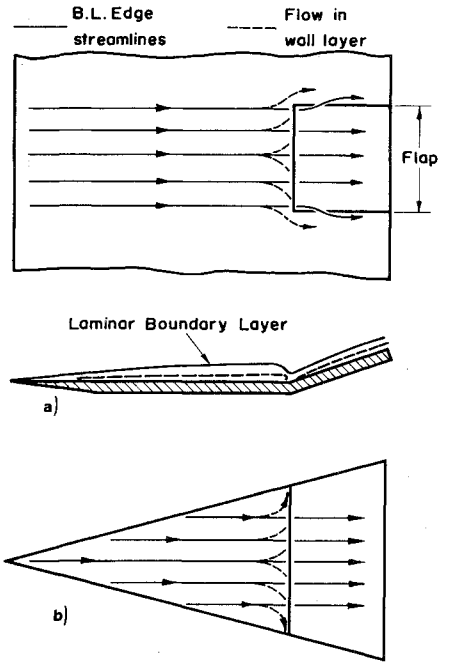

Fig. 3 Three-dimensional flow in laminar boundary-layer approaching flap.

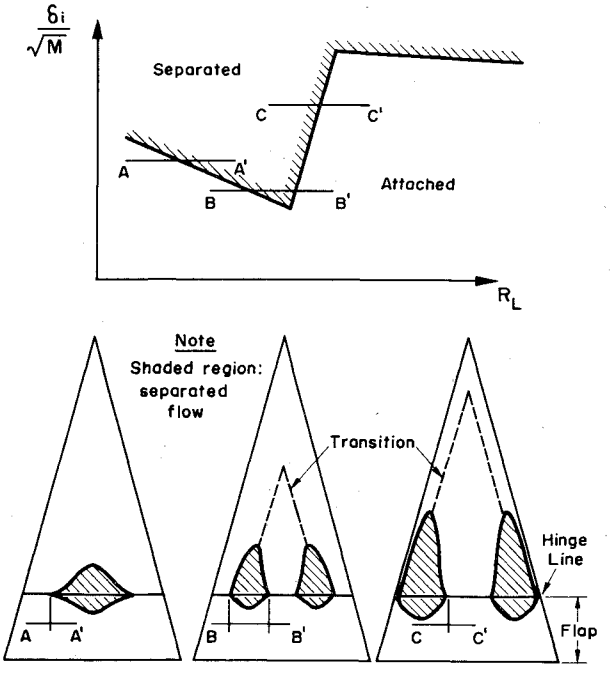

Fig. 4 Some flap-induced separation patterns on delta wing.

two-dimensional laminar flow[9] (also shown in Fig. 2). In the turbulent case, momentum exchange across the boundary layer precludes such a flow mechanism, and the delta wing boundary layer is, therefore, expected to behave in a more two-dimensional fashion at incipient separation, in accord with the present observation.

Flap-Induced Separation Patterns

The incipient-separation boundary for the delta wing (Fig. 2) was derived from center-line data. Application of these data on a two-dimensional strip theory basis to outboard locations permits the spanwise movement of the incipient separation to be predicted. As shown in Fig. 4, such an attempt qualitatively indicates typical cases with increasing

Reynolds number: a) A laminar separation bubble of limited spanwise extent first appears in the middle of the wing, with attached laminar flow on either side. b) Onset of transition in the wing boundary layer causes a local collapse of separation in the middle, while laminar separation persists outboard, producing a characteristic "two-lobed" separation pattern. c) The outboard lobes of laminar separation spread to the extremities of the hinge line, the inner (transitional or turbulent) flow remaining attached. The three examples illustrated in Fig. 4 have been observed in flow visualization studies reported in Ref. 1.

Conclusion

Trailing-edge flap-induced separation data on 75° delta wings have been examined to determine incipient separation characteristics. While the delta wing data for the turbulent boundary layer correlate with two-dimensional results, in the laminar and transitional cases a nearly parallel shift to higher flap angles for incipient separation is found. More data are needed (particularly for a range of leading-edge sweep angle) to establish properly the distinctive features of incipient separation on delta wings highlighted in this Note.

References

[1] Rao, D. M., "Hypersonic Control Effectiveness Studies on Delta Wings with Trailing-Edge Flaps," Ph. D. Thesis, Aeronautics Dept., Imperial College, London University, 1970.

[2] Davies, L., private communication (1970).

[3] Keyes, J. W., "Pressure and Heat Transfer on a 75° SweptDelta Wing with Trailing-Edge Flap at Mach 6 and Angle of Attack to 90°," NASA TN D-5418, Sept. 1969.

[4] Whitehead, A. H., Jr., and Keyes, J. W., "Flow Phenomena and Separation over Highly Swept Delta Wings with Trailing-Edge Flaps at Mach 6," *AIAA Journal*, Vol. 6, Dec. 1968, pp. 2380-2387.

[5] Johnson, C.B., "Pressure and Flowfield Study at Mach Number 8 of Flow Separation on a Flat Plate with Deflected Trailing-Edge Flap," NASA TN D-4308, March 1968.

[6] Needham, D. A. and Stollery, J. L., "Boundary-Layer Separation in Hypersonic Flow," AIAA Paper 66-455, Los Angeles, Calif., 1966.

[7] Rao, D. M., "An Experimental Study of the Hypersonic Aerodynamics of Delta Wings," *Journal of the Aeronautical Society of India*, Vol. 23, Nov. 1971, pp. 183-190.

[8] Stollery, J. L., "Laminar and Turbulent Boundary-Layer Studies at Hypersonic Speeds," ICAS Paper 72-09, International Council of Aeronautical Sciences, London, 1972.

[9] Putnam, L. E., "Investigation of Effects of Ramp Span and Deflection Angle on Laminar Boundary-Layer Separation at Mach 10.03," NASA TN D-2833, May 1965.

Postbuckling Analysis of Crossply Laminated Plates

Ramesh Chandra*
National Aeronautical Laboratory, Bangalore, India.

Nomenclature

a	= plate length in x direction
b	= plate width in y direction
w	= deflection of a point on median surface of plate in direction normal to the undeformed plate
E_L, E_T	= Young's moduli of lamina in parallel to fibre and perpendicular to fiber directions, respectively
G_{LT}	= shear modulus of lamina in LT plane
μ_{TL}, μ_{LT}	= Poisson's ratios; first subscript denotes lateral direction, second denotes load direction
E_f, E_m	= Young's moduli of fibre and matrix, respectively
m	= crossply ratio (ratio of the total thickness of odd layers to the total thickness of even layers)
n	= total number of layers
r	= a/b, aspect ratio of the plate
V_m	= volume content of matrix
P	= applied load
P_o	= buckling load
E	$= E_L$
F	$= E_T/E_L$
μ	$= \mu_{LT}$
η	$= G_{LT}/E_L$
δ	$= \eta(F-\mu^2)/F$
C_{11}	$= EF/(N-\mu^2)$
A	= amplitude of buckling mode

Received January 27, 1975; revision received April 1, 1975.
Index categories: Structural Composite Materials; Structural Stability Analysis.

*Scientist, Structural Sciences Division.

Introduction

POSTBUCKLING analysis of orthotropic plates is presented in Ref. 1. Chan[2] presented postbuckling analysis for arbitrarily laminated plates using energy methods. In this Note, an approximate solution (one term solution) to postbuckling problem of unsymmetrically stacked crossply laminated plate simply supported all over the edges is presented. The analysis is based on governing equations derived in Ref. 3.

Analysis

The governing equations for crossply laminated plates are obtained by deleting the inertia term from the governing equations of Ref. 3. These are recorded as follows:

$$L_1 w - L_3 \phi - L_n(\phi, w) = 0 \tag{1a}$$

$$L_2 \phi + L_3 w - \tfrac{1}{2} L_n(w, w) = 0 \tag{1b}$$

where ϕ is the Airy Stress Function.

$$L_1 = D_{11}^*(\partial^4/\partial x^4) + 2(D_{12}^* + 2D_{66}^*)(\partial^4/\partial x^2 \partial y^2) + D_{22}^*(\partial^4/\partial y^4)$$

$$L_2 = A_{22}^*(\partial^4/\partial x^4) + (2A_{12}^* + A_{66}^*)(\partial^4/\partial x^2 \partial y^2) + A_{11}^*(\partial^4/\partial y^4)$$

$$-L_3 = B_{21}^*(\partial^4/\partial x^4) + (B_{11}^* + B_{22}^*)(\partial^4/\partial x^2 \partial y^2) + B_{12}^*(\partial^4/\partial y^4)$$

$$L_n(\phi, w) = \phi_{,xx} w_{,yy} + \phi_{,yy} w_{,xx} - 2\phi_{,xy} w_{,xy}$$

A^*, B^*, and D^* are the matrices as defined in Ref. 4.

The plate is assumed to be simply supported at all the edges. The deflection function satisfying the geometric boundary conditions is assumed as follows:

$$w = A \sin(\pi x/a) \sin(\pi y/b) \tag{2}$$

It is not possible to satisfy the force boundary conditions by the previous function as the moment depends, not only upon the curvatures, but in-plane forces too, for unbalanced laminated plates. Hence, a modified galerkin's method[5] wherein the residues at the edges are minimized, is applied here.

Inplane boundary conditions considered are as follows:

$$\int_o^b (\phi_{,yy})_{x=o,a} dy = -P; \quad \int_o^b (\phi_{,xy})_{x=o,a} dy = o$$

$$\int_o^a (\phi_{,xx})_{y=o,b} dx = o; \quad \int_o^a (\phi_{,xy})_{y=o,b} dx = o \tag{3}$$